https://doi.org/10.5194/egusphere-2026-820
Preprint. Discussion started: 6 March 2026

Integrating total water level data and visual evidence to assess coastal flooding in San Diego County

Denali M. Pinto[1*], Antonio Catanzarite[1*], Anshul Govindu[1], Laura Engeman[1], Thomas W. Corringham[1], Julia Fiedler[2], Alexander Gershunov[1], Mark Merrifield[1]

[1]Scripps Institution of Oceanography, University of California San Diego, La Jolla, 92093, USA
[2]University of Hawaii, Manoa, 96822, USA

[*]These authors contributed equally

Correspondence to: Denali M. Pinto (d1pinto@ucsd.edu)

Abstract. Coastal flooding in Southern California poses a growing threat to communities and infrastructure, exacerbated by climate change and sea level rise. Total water level (TWL), the combination of sea level, tides, and wave runup, is increasingly used to forecast coastal flooding, but validating the thresholds at which flood impacts occur remains a challenge. This study examines the relationship between modeled TWL and photographic or video evidence of flooding in San Diego County from 2010 to 2024. We integrate model output from the Coastal Data Information Program with visual records from community monitoring programs to assess spatial and seasonal variations in flood occurrence. We also evaluate the influence of atmospheric rivers and El Niño conditions. Atmospheric river days were associated with an increase in the likelihood of observed flooding, and El Niño winters showed a positive but weaker correlation. Overall results demonstrate a robust but imprecise correlation between modeled TWL and observed flood impacts, with uncertainty driven largely by convenience sampling in the visual dataset. Despite these limitations, modeled TWL is shown to be a useful proxy for flood risk. Our findings underscore the need for systematic flood impact documentation to refine threshold estimates and improve flood forecasting and coastal management.

1 Introduction

On January 6, 2023, waves over three meters impacted the San Diego coastline. The event was associated with a series of atmospheric rivers which caused widespread flooding and coastal damage (NOAA-CNRFC, 2024; Preston, 2023). At the Del Mar nearshore buoy, part of the Coastal Data Information Program (CDIP), which monitors waves and tides, sensors captured the surge. In coastal communities across San Diego County, waves overtopped highways, flooded streets and parking lots, and scattered debris. As part of an ongoing citizen science effort, residents and researchers documented the impacts through photographs and videos, capturing flooding from Imperial Beach to Oceanside (Fig. 1).

https://doi.org/10.5194/egusphere-2026-820
Preprint. Discussion started: 6 March 2026

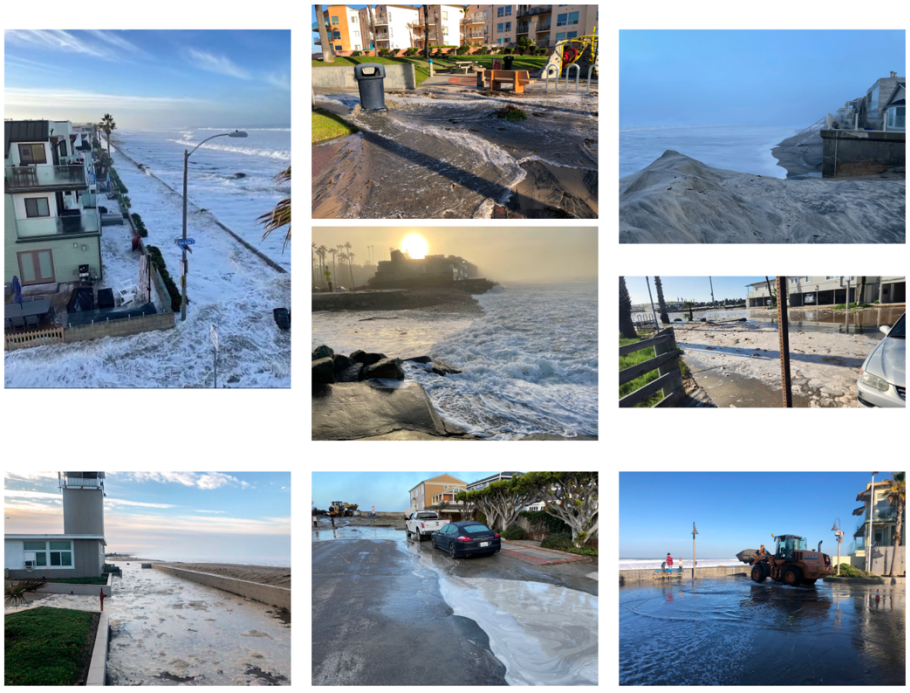

Figure 1. Flooding photographs from January 6, 2023, taken along the southern California coast from Imperial Beach through Oceanside.

For years, scientists have modeled total water level (TWL), the combined effect of tides, sea level, and wave runup, to predict coastal flooding in Southern California. Yet identifying the TWL thresholds at which modeled values correspond to real-world impacts, which we will refer to as "impact thresholds," remains a challenge. This study builds on these observations by linking over a decade of modeled TWL data with visual evidence to improve how we understand, monitor, and forecast coastal flood risks by quantifying impact thresholds at specific locations, using statistical methods.

Coastal flooding is an escalating global concern, driven by rising sea levels and intensifying storms associated with climate change. In San Diego County and Southern California, these risks extend beyond beachfront property to affect coastal infrastructure, public access to beaches, and the regional economy (OPC, 2024; Wing et al., 2022). Sea levels at the San Diego tide gauge have risen approximately 0.2 meters over the past century (OPC, 2024; OEHHA, 2024) and are projected to rise an additional 0.15 to 0.37 meters by 2050, and 0.6 meters by 2100 (Griggs et al., 2017; Merrifield et al., 2021; Younger, 2025). Seasonal high tides, or king tides, which currently produce predictable flooding in low-lying areas, serve as a proxy for understanding future sea level rise impacts (Ray & Merrifield, 2019; Thompson et al., 2021).

While still water level (SWL) data from tide gauges have traditionally served as indicators of minor coastal flooding days or hours (Sweet et al., 2018; Thompson et al., 2021), wave-driven processes can substantially increase water levels during storm events. Recent research has highlighted the importance of wave runup, a key component of TWL, in driving flooding events on the U.S. West Coast (Serafin et al., 2017). Despite TWL's growing use in flood prediction, few studies have directly

https://doi.org/10.5194/egusphere-2026-820
Preprint. Discussion started: 6 March 2026

linked modeled TWL data to qualitative evidence such as photographs and videos of flooding in southern California (e.g., Merrifield et al., 2021).

Forecasted TWL provides a critical advantage over tide gauges alone by capturing the dynamic, wave-driven processes that often determine whether flooding will reach onshore infrastructure. For emergency managers and coastal planners, having access to reliable TWL forecasts is not enough; they must also understand what specific TWL values mean in terms of likely impacts. They need to know impact thresholds: the modeled TWL levels at which tangible consequences such as flooded streets, debris on walkways, or damage to property are likely to occur. These thresholds vary by location and context, and can inform proactive decision-making, such as issuing warnings, placing sandbags, or mobilizing response crews. This study addresses that need by estimating impact thresholds for several locations in San Diego County using logistic regression to determine the TWL level at which photographic or video evidence of flooding becomes at least 50% likely. While this 50% threshold is used for interpretability, it could be adjusted depending on the stakes of a given decision, local tolerances for risk, or potential biases in the photographic record. In this way, the approach supports flexible, evidence-informed flood preparedness across a range of coastal contexts.

This study integrates modeled TWL estimates with photographic and video records of flooding events across San Diego County from 2010 to 2024. By analyzing maximum daily TWL values and correlating them with observed flood impacts, we estimate the TWL impact thresholds, levels at which damaging flood impacts become likely along different parts of the coast. Our findings reveal seasonal and spatial patterns of flooding, demonstrate the influence of wave-driven processes beyond still water levels alone, and provide actionable insights to improve flood forecasting and inform adaptation strategies for vulnerable coastal communities.

2 Materials and Methods

This study integrates quantitative modeled total water level (TWL) data with qualitative photographic and video evidence to assess flooding impacts in San Diego County from 2010 to 2024 and to quantify flood impact thresholds, values of modeled TWL that are most likely to be associated with physical flood impacts as documented in photographic and video records. For convenience we use the term “photos” to refer to both photographic and video records of coastal flooding. The main analysis focuses on identifying temporal patterns, spatial distributions, and quantifying flood threshold values by location. We also explore the impact of meteorological climatological factors in generating elevated modeled TWL values and observed coastal flood impacts, including atmospheric rivers and the El Niño Southern Oscillation (ENSO) interannual mode of climate variability.

1.1 Collection of Photo Evidence

Photo evidence was gathered from multiple sources, including research groups at Scripps Institution of Oceanography (SIO), community science platforms, and social media (Fig. 2). Primary sources, provided in Supplementary Materials, included:

https://doi.org/10.5194/egusphere-2026-820
Preprint. Discussion started: 6 March 2026

- SIO Flood Documentation Repository: a shared database for researchers to upload flood observations;
- Coastal Flooding Viewer: maintained by the SIO Coastal Processes Group (CPG), which compiles researcher-contributed flood observations;
- Stormphoto Database: formerly hosted by the Coastal Data Information Program (CDIP), with public and student photo submissions;
- California King Tides Project: a citizen science gallery documenting flooding events (California King Tides Project, 2025);
- Social media and news outlets, including Instagram and YouTube, searched using relevant terms (e.g., "San Diego coastal flooding," "king tides").

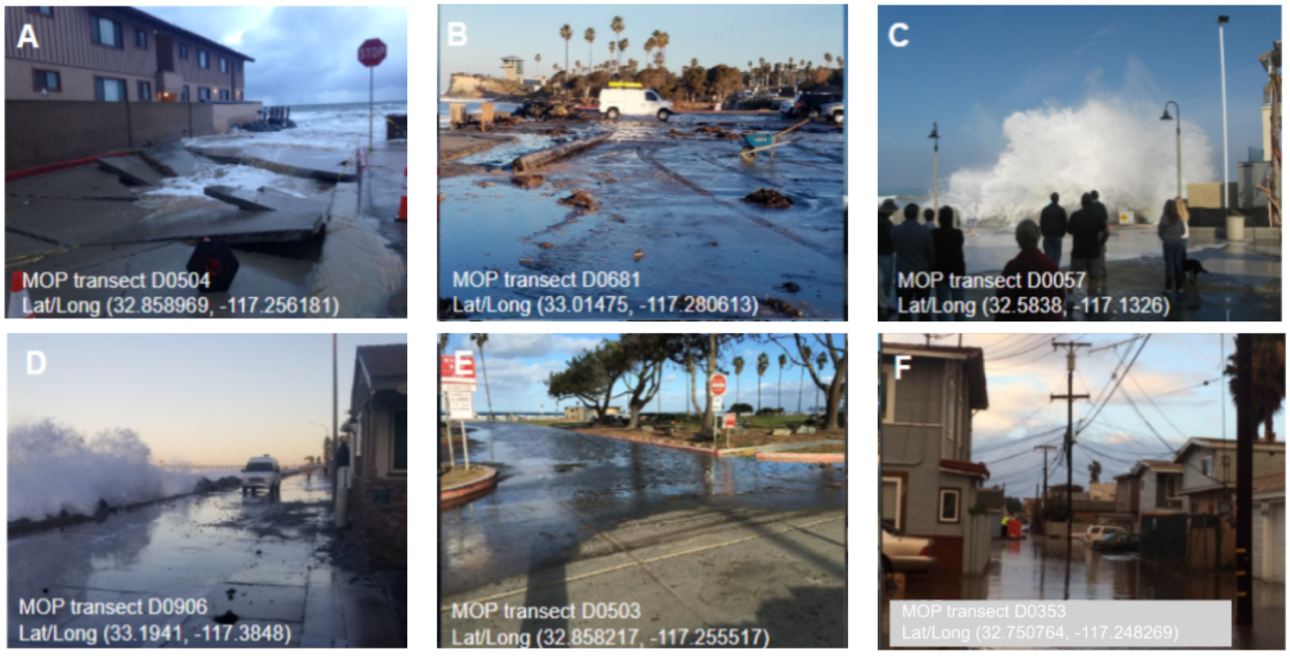

Figure 2. (A) La Jolla Shores, 7 January 2016; (B) Cardiff, 11 January 2021; (C) Imperial Beach, 31 January 2010; (D) Oceanside, 26 January 2021; (E) La Jolla Shores, 25 November 2015; (F) Ocean Beach, 6 January 2016. Each event illustrates flooding impacts recorded through photographic evidence, highlighting variability in location and timing across the region.

Each photo was reviewed to confirm that it depicted flooding requiring cleanup or other significant response. Notes from original contributors, such as "concrete" for paved flooding, "seafoam," or "stones washed ashore," were retained but not used in our analyses. Records were organized chronologically and spatially, matched to the nearest CDIP Monitoring and Prediction (MOP) transect (O'Reilly et al., 2016). MOP transects are spaced every 100 meters along the California coast. Duplicate submissions for the same transect and date were consolidated. For each transect-day combination, we constructed a binary indicator to classify whether photo evidence of coastal flooding was present. This dataset provided localized insights into the severity and spatial extent of flooding, complementing quantitative TWL data. In the City of Imperial Beach, the

https://doi.org/10.5194/egusphere-2026-820
Preprint. Discussion started: 6 March 2026

southernmost city in California, bordering San Diego Bay to the north, the Tijuana River Estuary to the east, Mexico to the south, and the Pacific Ocean to the west, photographs indicating flooding from the estuary were removed to focus exclusively on coastal flooding. As there were no photo records of flood impacts within San Diego Bay or Mission Bay, all of our photos documented coastal flooding and not back bay flooding or flooding due to groundwater intrusion.

1.2 Total Water Level Data

Modeled TWL data were obtained from CPG and CDIP at SIO. Wave data were sourced from CDIP buoys, and beach slope data necessary for modeling wave runup were provided by CPG. Wave runup was calculated using the Stockdon method (Stockdon et al., 2006), combining buoy data with local beach slopes derived from satellite imagery using CoastSAT. Sea level and tidal data came from NOAA's La Jolla tide gauge. TWL data are available from January 2000 to the present, however given the scarcity of flood impact photos before 2010, we chose to focus our analysis on the period from January 2010 to April 2024, a period covering 14 extended fall and winter periods (October–March).

Hourly tide, runup, and TWL data were aggregated into daily maximum TWL, daily maximum runup, and daytime-specific maximum values, from 7:00 a.m. to 6:00 p.m., inclusive (more precise daytime filtering did not meaningfully alter results on a preliminary analysis of a subset of the data). TWL values from one and two days prior were also included. TWL was calculated as the sum of wave runup and tidal levels, integrating both oceanographic and coastal geomorphic factors. Each data point was linked to its corresponding MOP transect and date. The data included 51 MOP transects from the southern border of San Diego County with Mexico to the north border with Orange County. Coronado island transects and transects without photographic evidence of flooding were excluded from the analysis. The data included 3,421 days, yielding 167,301 transect-day pairs. There were 283 transect-days with photographic evidence of flooding.

1.3 Linking Photos to TWL Data

TWL data were matched to the MOP transects corresponding to each photo. The MOP system, operated by CDIP, monitors coastal waves and sand levels at regional scales. Directional wave buoys generate a high-resolution spectral wave model (CDIP MOP Introduction, 2025), accounting for island blocking, refraction, and shoaling. Latitude and longitude coordinates from photos were used to assign transects. For photos where only general location descriptions were available (e.g., "Cardiff parking lot"), midpoint coordinates were used to link to a specific MOP transect. By aligning TWL measurements with visual flood documentation by transect and date, we evaluate the correlation between modeled TWL and observed flooding impacts.

1.4 Data Analysis and Statistical Modeling

All analyses were conducted in R (R Core Team, 2025; data and code are publicly available). Visualizations and statistical models illustrate relationships between TWL, photo evidence, and external climatic drivers. Time series plots illustrate daily maximum TWL values and recorded flooding events, revealing seasonal and annual variability. Histograms capture monthly

https://doi.org/10.5194/egusphere-2026-820
Preprint. Discussion started: 6 March 2026

flooding frequencies, highlighting king tide seasonality and possible influences from El Niño and atmospheric rivers (ARs). Geographic flood patterns were mapped using ArcGIS Pro (Esri, 2025).

1.5 Logistic Regression Models and Density Plots

Logistic regression models were used to estimate the probability of photographic flood evidence as a function of six variables whose names are presented here with their descriptions:

- TWL: daily maximum total water level.
- Runup: daily maximum wave runup.
- TWL-daytime: daytime (7 a.m.–6 p.m.) maximum TWL.
- Runup-daytime: daytime maximum runup.
- TWL-max: maximum TWL on the photo date or preceding day.
- TWL-max-daytime: maximum daytime TWL on the photo date or preceding day.

For each model, the TWL threshold corresponding to a 50% probability of photo evidence was identified, providing an estimate of the TWL level above which flooding was more likely to be documented than not. Model performance was evaluated using *p*-values for significance and Akaike Information Criterion (AIC) for model fit. The data were also used to generate density plots at each MOP transect for which there were multiple photo-days to illustrate the distribution of TWL values for days with and without photo evidence.

1.6 Climatic Driver Assessment

To examine potential climatic influences, atmospheric river (AR) and El Niño-Southern Oscillation (ENSO) data were matched to the modeled TWL and observational photo records. AR data were obtained from the Gershunov et al. (2017) AR catalog updated through July 2023 (WECLIMA SIO R1 AR Catalog). ENSO phases (El Niño, La Niña, neutral) and sea surface temperature anomalies were drawn from the Oceanic Niño Index (ONI V2; Bamston et al., 1997) for the Niño 3.4 region.

These variables were included in statistical models to assess their relationship with TWL values and photo evidence of flooding. While SWL indicators from tide gauges have traditionally been used to estimate minor flooding (Sweet et al., 2018; Thompson et al., 2021), previous studies have shown that wave-driven processes, especially wave runup, significantly influence water levels during storm events on the U.S. West Coast (Serafin et al., 2017), hence the focus on linkages between TWL and qualitative flood evidence in this study.

https://doi.org/10.5194/egusphere-2026-820
Preprint. Discussion started: 6 March 2026

3 Results

3.1 Temporal Variability of Coastal Flooding

Photo evidence of coastal flooding reveals clear seasonal and interannual patterns. Flooding events were most frequent from November to February, aligning with higher TWL values during winter months. January consistently showed the highest number of flooding events, with over 150 photo-documented occurrences, more than double the number recorded in December (Fig. 3).

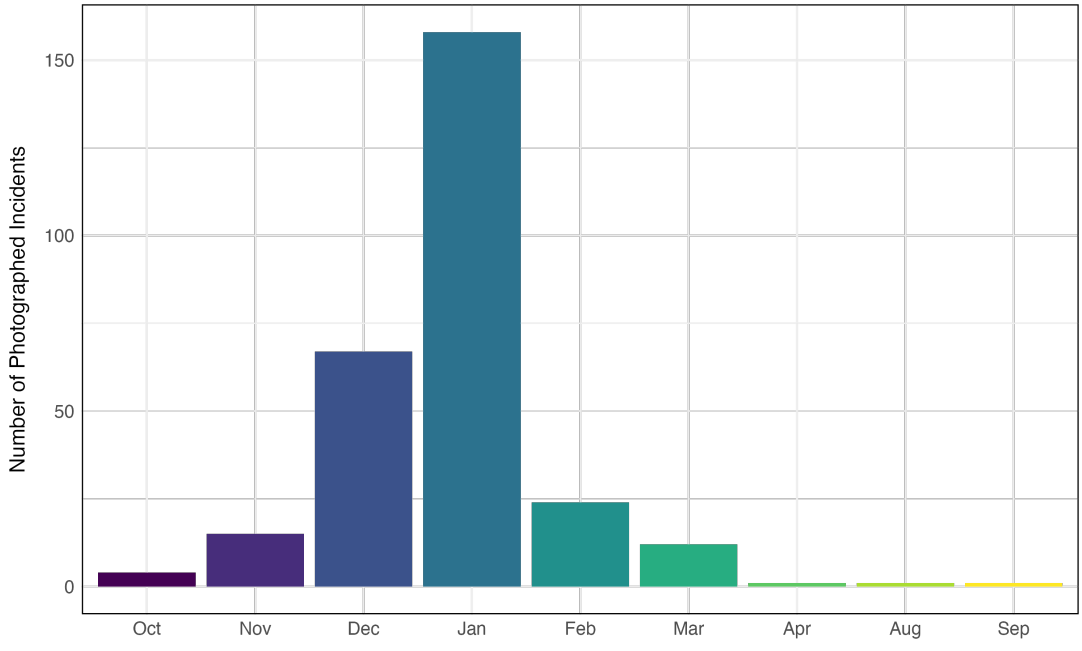

Figure 3. Monthly variation in visually documented flooding events from 2009 to 2024.

No flooding photos were recorded from May through July, with minimal evidence in April, August, and September. These patterns closely match previous observations of king tide seasonality and winter flooding peaks (Flick, 1998). Interannual variability was also evident. Flooding was most intense in 2019, 2021, and 2023, with January 2021 alone accounting for approximately 50 documented events (Fig. 4). We included records from the 2009–2010 and 2013–2014 extended fall and winter seasons. There were few photos in these seasons and a gap in photographic evidence between 2010 and 2013, however, the impact thresholds were not significantly different in excluding these years. Thus, we included all photo records from 2010–2024.

https://doi.org/10.5194/egusphere-2026-820
Preprint. Discussion started: 6 March 2026

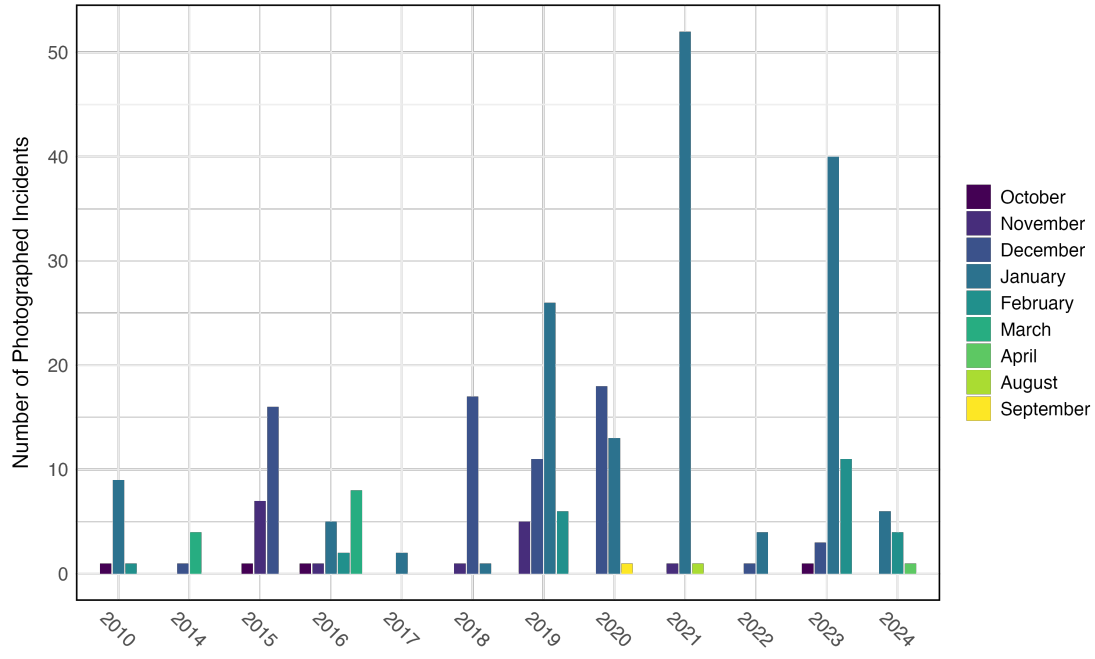

Figure 4. Annual variation in the number of visually documented flooding events from October 2009 to April 2024. Each bar represents a month within the year, highlighting months with visual records of coastal flooding.

3.2 Spatial Variability of Coastal Flooding

The number of documented flood impacts by MOP transect varied widely along the San Diego County coastline (Fig. 5). Photo hotspots included Imperial Beach, La Jolla, and Cardiff State Beach. Imperial Beach accounted for over 170 days with photo evidence, comprising 60 percent of the 283 total recorded events. Cardiff and La Jolla had 35 and 20 days with photo evidence, respectively.

https://doi.org/10.5194/egusphere-2026-820
Preprint. Discussion started: 6 March 2026

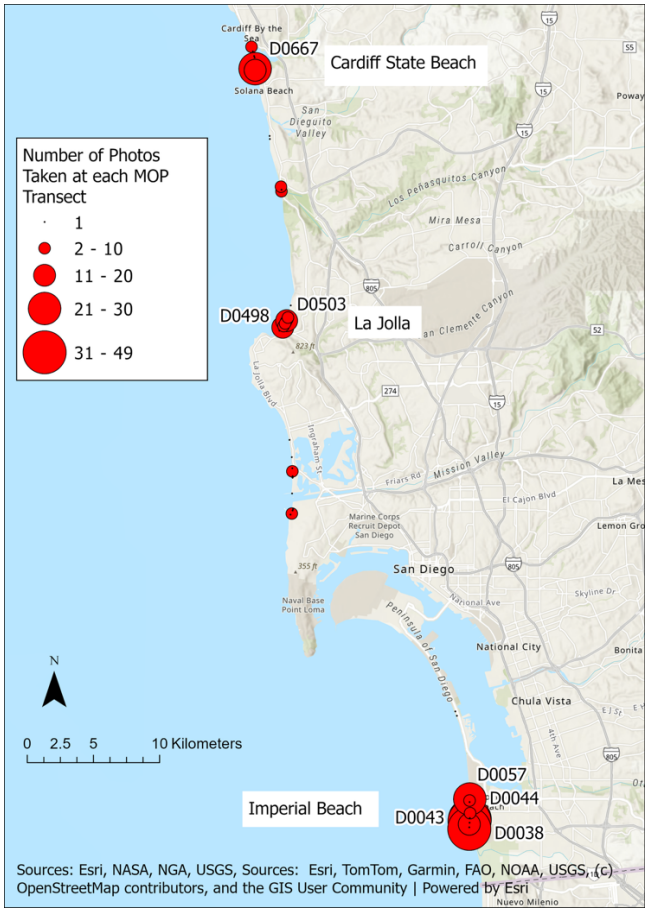

Figure 5. Map of the southern California coast using OpenStreetMap as the base layer in ArcGIS Pro (Version 3.4.0; Esri, 2025), showing the quantity of visually documented flooding events per location between 2015 and 2024. Circle size is proportional to the number of recorded flooding events.

Three transects in Imperial Beach (D0044 and D0043 between Cortez Avenue and Descanso Avenue along Seacoast Drive, and D0038 at the southern end of Seacoast Drive) had the highest frequency of visual flood impact documentation, each transect with over 30 photo documented flooding events. D0044 (between Cortez Avenue and Descanso Avenue) was the most active, with 46 days of flooding recorded between 2010 and 2024. Seacoast Drive runs north-south along the Pacific coast, west of the Tijuana River Estuary, with roads and residential structures at risk of coastal and estuarine flooding. In this study we focus exclusively on coastal flooding, excluding any photographs of flooding to the east of Seacoast Drive. The vast majority of MOP transects in the county were associated with no photographic evidence of flooding. Of the 49 unique MOP transects in the county with at least one documented event, only eight had 10 or more flooding events; 28 transects recorded a single flood event (Fig. 6).

https://doi.org/10.5194/egusphere-2026-820
Preprint. Discussion started: 6 March 2026

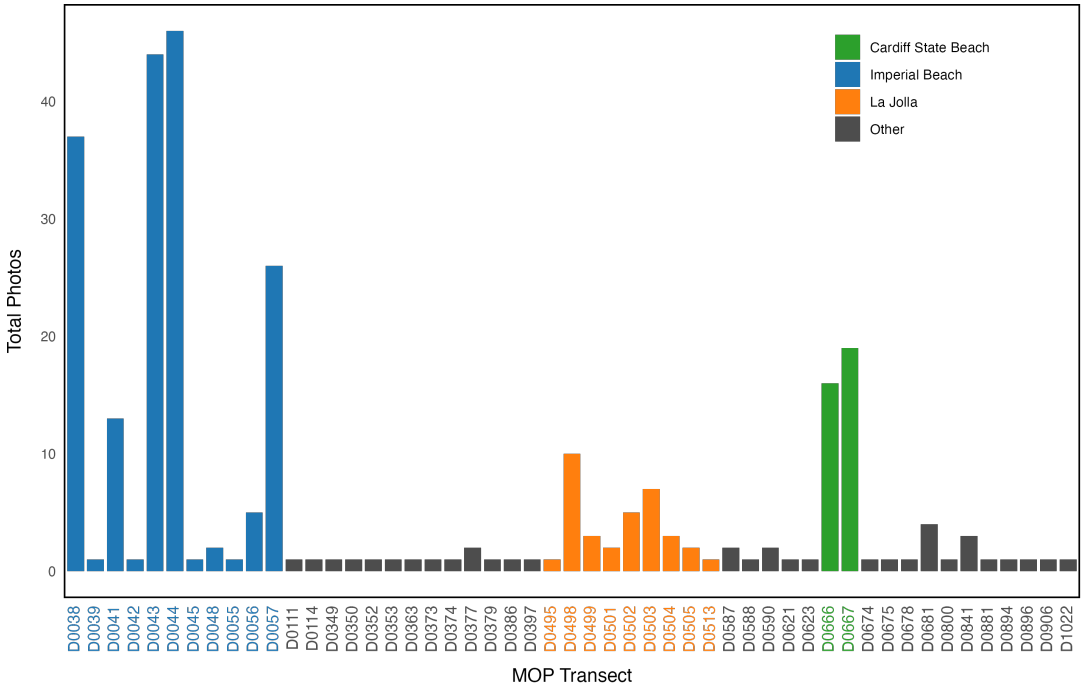

Figure 6. Number of days with visual evidence of flooding recorded per MOP transect in the dataset.

The spatial variability in photographic documentation likely reflects both actual flooding dynamics and variations in monitoring intensity. Researchers from Scripps Institution of Oceanography (SIO) often targeted Imperial Beach during high-flood predictions, increasing the number of documented events in that area (Xia, 2023). Data collection biases related to accessibility, observer presence, and timing, such as under-documentation of nighttime events, also contributed to uneven spatial coverage.

3.3 Relationship Between Photo Evidence and Total Water Level: Impact Thresholds

Over the study period, photo evidence generally coincided with days with elevated modeled TWL values. In Imperial Beach's well documented D0044 transect, most flooding photos aligned with TWL peaks (Fig. 7). Coastal flood photos were most strongly correlated with the TWL-max-daytime metric, which incorporates the highest daytime TWL across two consecutive days (Fig. 8). Instances where photo evidence and TWL did not align were rare and typically occurred on days with lower TWL which in some cases may have been due to data entry errors or mismatches in timing between flooding and photo capture.

https://doi.org/10.5194/egusphere-2026-820
Preprint. Discussion started: 6 March 2026

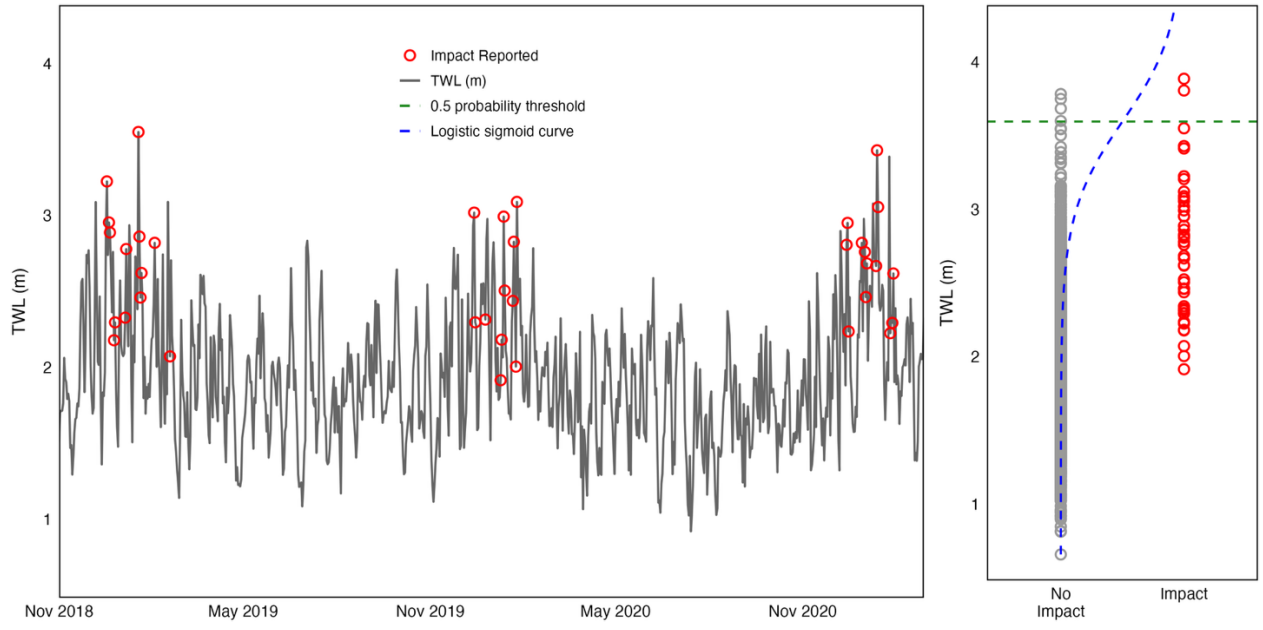

Figure 7. Relationship between visually documented flooding events and TWL at MOP transect D0044 (Lat: 32.5732 N, Long: -117.1490 W) along Seacoast Drive in Imperial Beach, CA. Red dots on the time series (left) indicate dates with visually documented flooding events. Corresponding dates are categorized as "Impact" in the scatter plot (right), dashed blue line represents logistic sigmoid curve, horizontally dashed green line shows 0.5 probability threshold.

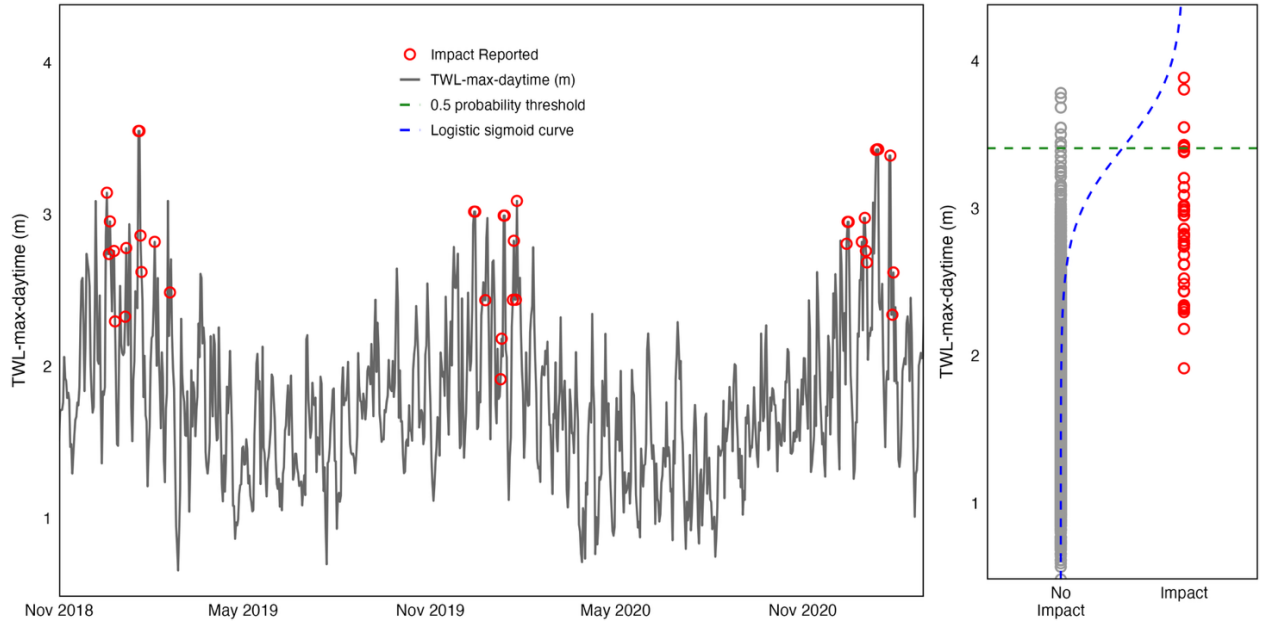

Figure 8. Relationship between visually documented flooding events and TWL-max-daytime at MOP transect D0044 (Lat: 32.5732 N, Long: -117.1490 W) along Seacoast Drive in Imperial Beach, CA. Red dots on the time series (left) indicate dates with visually documented flooding events. Corresponding dates are categorized as "Impact" in the scatter plot (right), dashed blue line represents logistic sigmoid curve, horizontally dashed green line shows 0.5 probability threshold.

https://doi.org/10.5194/egusphere-2026-820
Preprint. Discussion started: 6 March 2026

Logistic regression analyses to quantify impact thresholds confirmed that higher modeled TWL was associated with an increased likelihood of photo-documented flooding. For example, at D0038, the southernmost point on Seacoast Drive, the TWL threshold where photos were equally likely to occur or not was estimated at 3.54 meters (95% CI: 3.33-3.75 meters) relative to mean sea level. Daytime TWL outperformed 24-hour TWL as a predictor, likely because most photos were taken during daylight hours. Runup and daytime runup were less effective predictors. Introducing TWL-max (peak TWL on the photo day or previous day) and TWL-max-daytime variables improved model performance by addressing potential timing mismatches; in some cases, flood evidence may have been photographed the day after peak water levels occurred. TWL-max-daytime emerged as the most consistent predictor, yielding an impact threshold of 3.39 meters (95% CI: 3.23-3.56 meters) for transect D0038 with reduced model uncertainty relative to other predictors (Fig. 9).

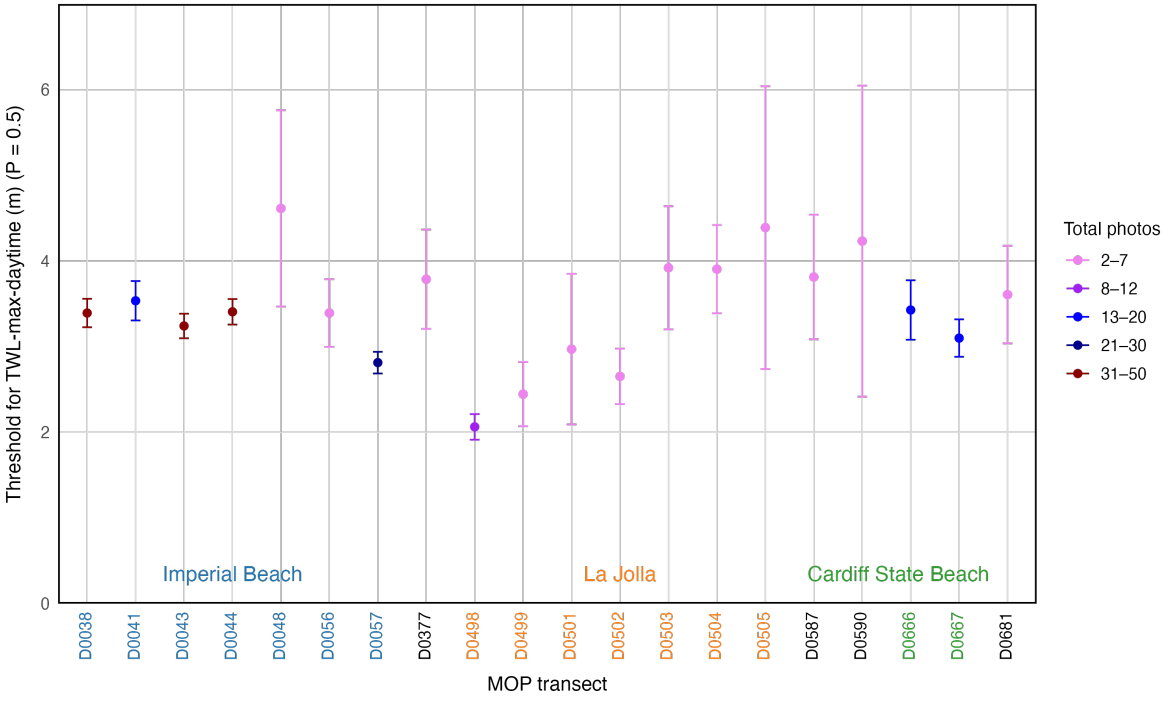

Figure 9. TWL-max-daytime as the predictor variable for photo evidence of flooding across MOP transects with more than one photo. Points represent threshold values, error bars indicate standard error, and colors correspond to the number of photographs recorded for each MOP transect. MOP transects for specific locations: Imperial Beach, La Jolla, and Cardiff State Beach are blue, orange, and green, respectively.

At least one photo documented flood event was observed at 49 separate MOP transects. Across these 49 San Diego County transects, the mean threshold and standard deviation were approximately 3.92 ± 1.13 meters, with a median of 3.74 meters (IQR: 3.38-4.39 meters). We also applied the logistic regression approach to the 21 transects with two or more flooding photos, excluding 28 transects with only a single documented flood day. For these 21 transects, the mean TWL-max-daytime (peak TWL over the photo day during daytime and the previous day) threshold was 3.69 ± 1.31 meters, with a median of 3.43

https://doi.org/10.5194/egusphere-2026-820
Preprint. Discussion started: 6 March 2026

meters (IQR: 3.10-3.91 meters). Transects with more extensive photo documentation yielded narrower error margins, underscoring the value of increased visual flood evidence data collection (Fig. 9).

To complement the logistic regression results, we fit Bayesian logistic models to estimate TWL-max-daytime thresholds corresponding to a 50% probability of photo-documented flooding. Weakly informative Normal(0, 2.5) priors were specified for intercept and slope parameters on the logit scale. Predictors were centered at 3.4 meters to improve computational stability. For transect D0038, the median Bayesian threshold was 3.42 meters, with a 95% credible interval of [3.27, 3.64]. Across all transects with at least two flood photos, the median countywide threshold was 3.68 meters [2.09, 14.47]. The wide credible interval reflects substantial uncertainty at transects with limited photo documentation, where posterior threshold estimates are weakly constrained by the data. The Bayesian framework explicitly propagates uncertainty in both slope and intercept parameters, leading to wider credible intervals at sparsely documented transects where the logistic slope is weakly identified. In contrast, transects with at least eight flooding photos exhibited narrower credible intervals, reflecting greater statistical confidence (Fig. 10). Results were qualitatively unchanged under moderately stronger priors (Normal(0, 1.5)).

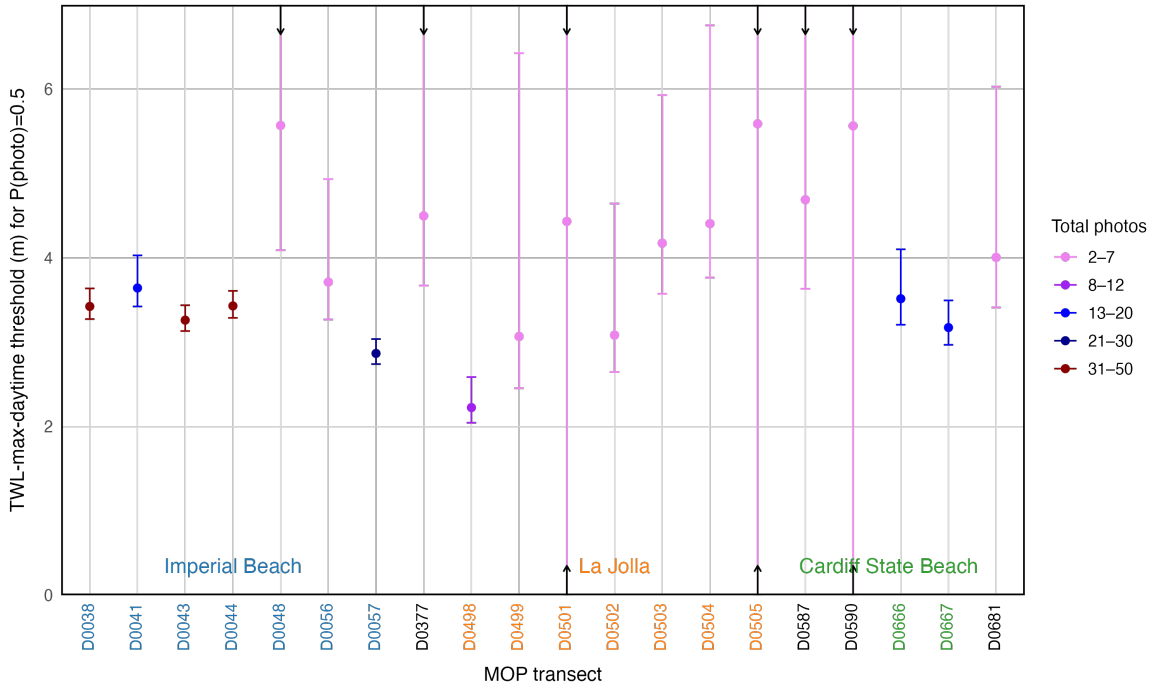

Figure 10. TWL-max-daytime as the predictor variable for photo evidence of flooding across MOP transects with more than one photo. Points represent median threshold values from a Bayesian model, error bars indicate the 95% credible interval, and colors correspond to the number of photographs recorded for each MOP transect. MOP transects for specific locations: Imperial Beach, La Jolla, and Cardiff State Beach are blue, orange, and green, respectively.

Among transects with at least eight flooding photos, the median threshold was 3.33 meters [2.14, 3.86], more closely aligned with the logistic regression results. These Bayesian estimates complement the regression-derived thresholds and

https://doi.org/10.5194/egusphere-2026-820
Preprint. Discussion started: 6 March 2026

quantify the uncertainty associated with varying data coverage. The results suggest that threshold uncertainty may be driven by data sparsity. Density plots of TWL values with and without photo evidence support the regression findings (Fig. 11).

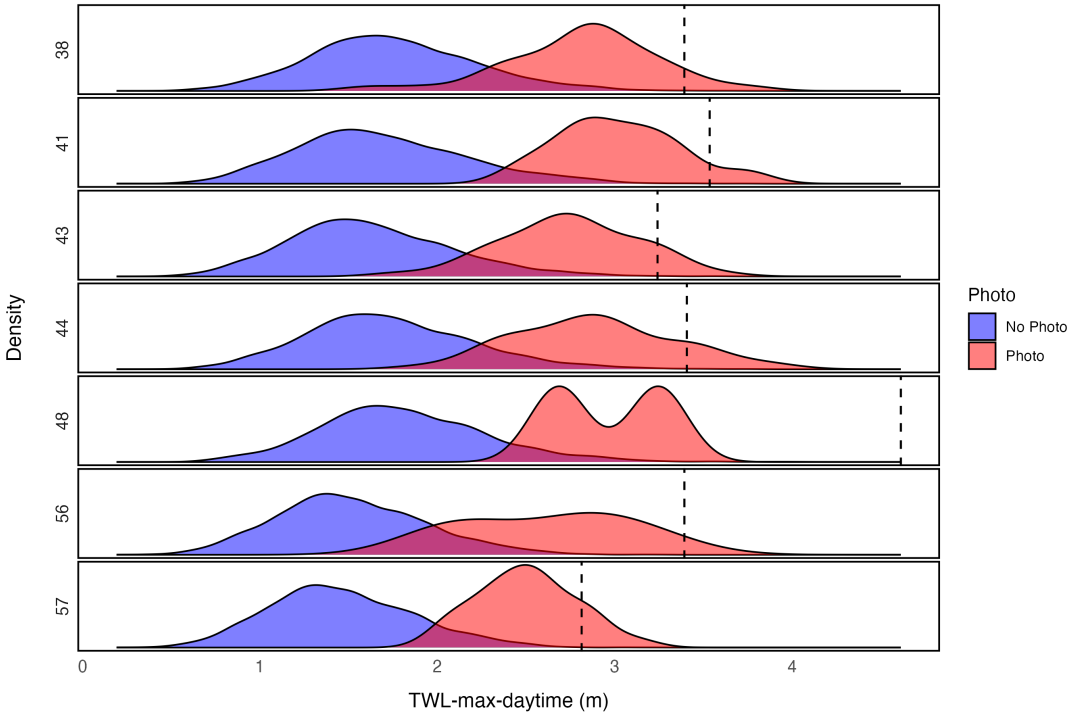

Figure 11. Density plots relating to MOP transects in Imperial Beach, CA. Dashed vertical lines correspond to TWL-max-daytime 0.5-probability thresholds from the logistic regression analysis. Note that these thresholds do not align with the density intersection points because there are many more observations without photos than with photos.

Photographed flood impact events generally occurred at higher TWL values, with clear separation between the distributions of TWL values for days with photo evidence and those without at all MOP transects.

While pooling MOP transects provides increased statistical power, the impact thresholds at individual transects are likely to be of greater value to stakeholders and decision makers. Anecdotally, city planners and coastal managers in San Diego's eight coastal municipalities (the cities of Oceanside, Carlsbad, Encinitas, Solana Beach, Del Mar, San Diego, Coronado, and Imperial Beach) reported that water levels of over 3.5 meters were cause for concern, providing modest confirmation of our modeling approaches.

3.4 Impacts of Atmospheric Rivers

Atmospheric river (AR) events in San Diego County primarily occur during winter months, coinciding with the seasonal patterns of flooding observed in this study. To assess their influence, we used the SIO R1 AR catalog (Gershunov et al., 2017) and calculated two AR intensity metrics: StormRank and LatRank, both based on the Ralph et al. (2019) AR ranking scheme which ranks storms on a scale of 1–5 based on their intensity and duration. StormRank captures the maximum AR rank over

https://doi.org/10.5194/egusphere-2026-820
Preprint. Discussion started: 6 March 2026

the duration of the storm as it moves up and down the coast. LatRank captures the maximum AR rank of the storm in the 32.5°N grid cell, corresponding to San Diego County.

Linear regression showed that AR events were associated with an average increase in TWL of approximately 0.13 meters with a one-day lag ($p < 0.001$). Model R^2 for this simple model was very low, however, with AR incidence accounting for less than one percent of TWL variance, suggesting that other factors, such as tides, wave heights, and storm surge, play much larger roles in TWL variability. A linear mixed-effects model accounting for variability across MOP transects produced similar results, with a 0.13-meter TWL increase observed within a one-day window post AR landfall.

To test the significance of AR association with photographic flood evidence, we compared 117 days with photo-documented flooding to 111 days with AR events. Only 10 days overlapped. A contemporaneous logistic regression at MOP transect D0038 showed no significant relationship, possibly due to timing mismatches between AR peaks and when flood impact photos were taken. Introducing temporal lags revealed stronger associations. The highest odds ratio (3.2, $p < 0.005$) occurred within a three-day post-landfall AR window, indicating that AR events increased the likelihood of photo-documented flooding threefold within three days after an AR makes landfall. Significant effects were also found for two- to six-day lags.

A generalized linear mixed model (GLMM) across transects indicated that AR events with a three-day lag increased the likelihood of flooding photos nearly fourfold (Fig. 12). This temporal offset may reflect the nature of stronger ARs, which frequently persist over multiple days, coupled with the tendency for photographs to be taken up to a day after flooding occurs. As a result, the peak in photographic evidence two to three days following initial AR landfall likely captures both the extended duration of impactful AR events and a lag in documentation timing.

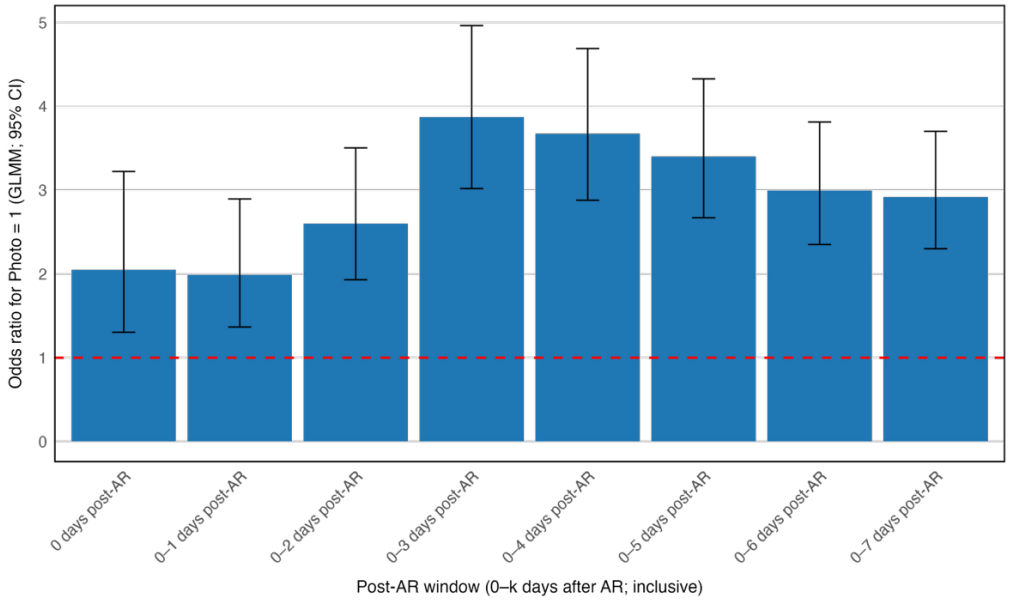

Figure 12. Effect of atmospheric river events on the likelihood of photos: output odds ratio from GLMM model. The odds ratio of the likelihood of photo evidence compared to the number of days post-AR event. The error bars represent 95% confidence intervals for the odds-ratios. If the confidence interval crosses one the effect is not statistically significant at the 0.05 level. The red dashed line corresponds to the reference line for an odds ratio of one which is where there is no effect.

https://doi.org/10.5194/egusphere-2026-820
Preprint. Discussion started: 6 March 2026

These findings suggest that ARs may contribute to flooding with a delayed response, consistent with the timing of flood impacts and the tendency for photos to be captured after water recedes. However, because of the small number of overlapping AR and photo days, these conclusions must be interpreted with caution. Previous studies have also reported an association between ARs and high-tide flooding along the U.S. West Coast, attributed to AR-driven wind, pressure, and rainfall effects (Piecuch et al., 2022). Future investigation could consider the role of beach orientation relative to AR orientation on TWL and incidence of photo documentation of flood impacts and a more detailed analysis of the timing of AR landfall versus the timing of coastal flooding impact photos.

3.5 Relationship with ENSO

The El Niño–Southern Oscillation (ENSO) influences tropical rainfall and wind patterns globally, with El Niño phases typically bringing wetter, cooler conditions to Southern California and raising sea levels through coastally trapped Rossby waves and intensified Pacific cyclones (Luna–Niño et al., 2025; Tseng & Johnson, 2022). La Niña phases are generally associated with warmer, drier winters in Southern California (Lindsey, 2017).

ENSO phases were categorized using the Oceanic Niño Index (ONI) (Barnston et al., 1997) for the Niño 3.4 region. Time series data from MOP transect D0038 showed that extreme TWL values (greater than 3.4 meters) occurred more frequently during El Niño phases than during La Niña or neutral phases (Figs. 13 and 14), suggesting a possible ENSO influence on flood conditions.

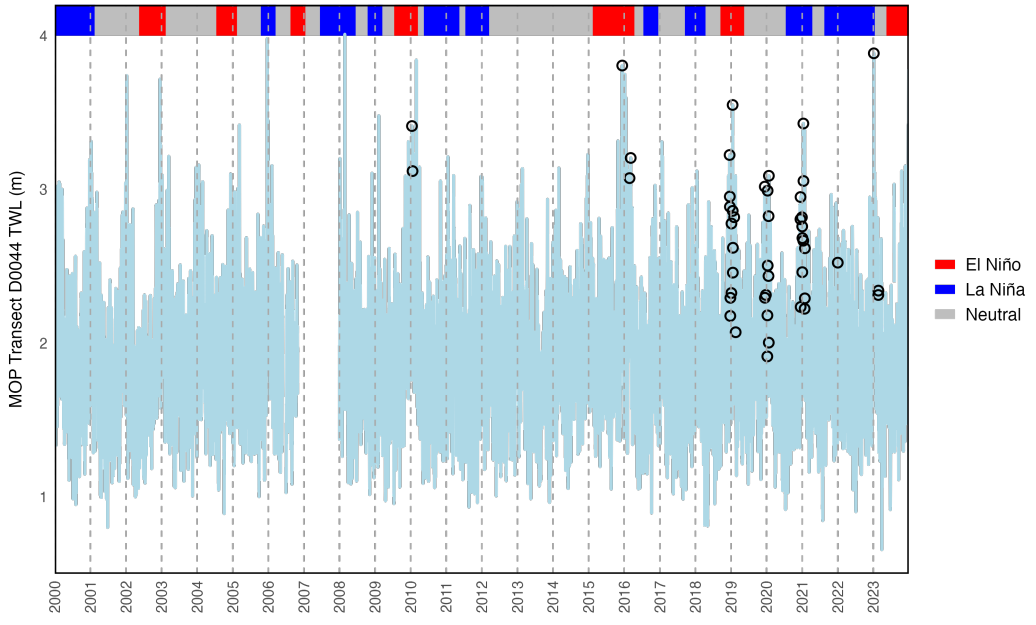

Figure 13. Maximum daily TWL values from MOP transect D0044 in Imperial Beach, CA. ENSO cycles are from the values obtained in the ONI V2 dataset. Grey circles indicate when photo evidence was obtained.

https://doi.org/10.5194/egusphere-2026-820
Preprint. Discussion started: 6 March 2026

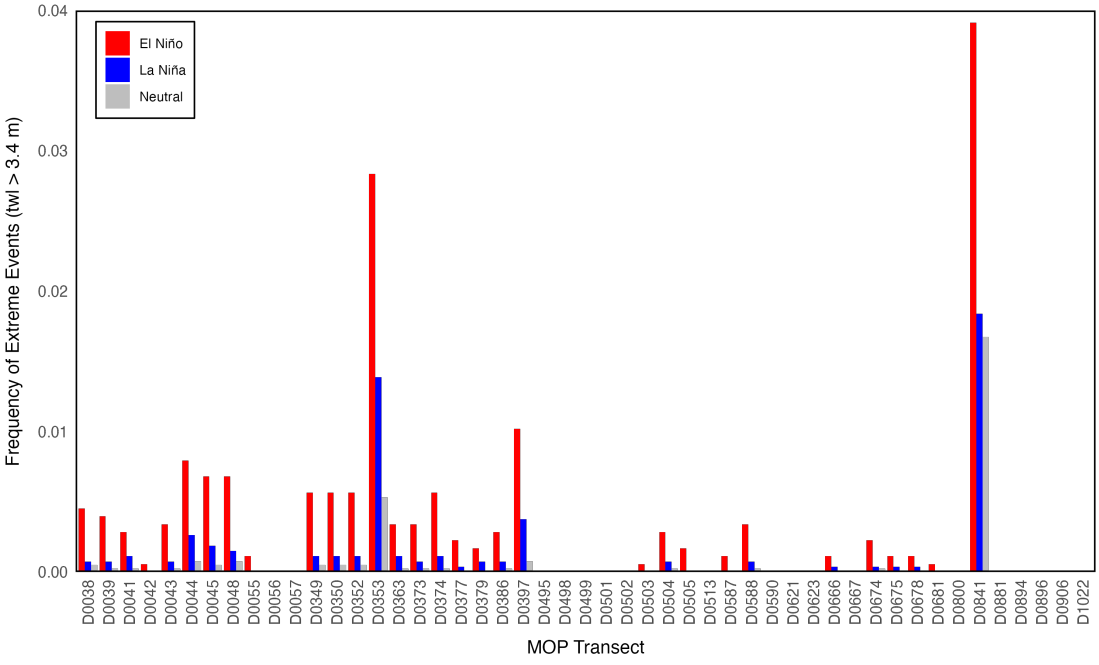

315 **Figure 14. Frequency of extreme TWL values (>3.4 meters) per MOP transect and their corresponding ENSO phases from 2000-2024. Examining MOP transects with at least one photo.**

However, the relatively short observational window (2010–2024) limits the analysis. Only one extreme El Niño event occurred during the study period (2015–2016), and ENSO operates on two- to seven-year cycles, with El Niño and La Niña events often separated by a year or more. While the broader TWL dataset (2000–2024) shows a stronger correlation between
320 extreme TWL peaks and El Niño phases, the overlap with photographic flood evidence remained limited.

The complexity of ENSO's interactions with AR events, precipitation, and coastal wave dynamics further complicates interpretation. While the data suggest that El Niño phases may elevate flood risks, longer-term analyses covering multiple ENSO cycles would be necessary to confirm these patterns.

3.6 Data Limitations

325 Interpretation of these climatic drivers is constrained by the reliance on convenience sampling for photographic flood evidence. Certain transects were observed more frequently than others, and data collection was biased toward daytime and accessible locations. Many impactful flooding events likely occurred without photographic documentation, and the timing of photos may not have aligned precisely with flooding peaks. While these biases introduce uncertainty into the analysis, they are consistent with known limitations of community-science data collection efforts.

330 Despite these constraints, the statistical associations observed, particularly the lagged relationship between ARs and flooding photos, provide valuable insights. They highlight the importance of considering lagged climatic influences and of integrating both hydrodynamic and atmospheric data into flood risk assessment. Future studies would benefit from expanded

https://doi.org/10.5194/egusphere-2026-820
Preprint. Discussion started: 6 March 2026

and standardized data collection protocols, including automated monitoring systems and more systematic community science engagement. Randomized or continuous photo sampling could reduce biases and improve alignment between observed flooding events and TWL measurements, enabling more accurate modeling of climatic drivers and flood thresholds.

4 Discussion

The spatial and temporal distribution of flooding captured in photographs and videos corroborates the modeled TWL data, reinforcing the validity of the findings and demonstrating the accuracy of existing tools in documenting varying intensities of coastal flooding. This integration of photo evidence with quantitative data enhances our understanding of flooding dynamics and validates coastal flooding measurements.

While efforts like flood documentation, reporting, and community engagement are important steps toward flood resilience, implementing comprehensive solutions remains a challenge. Continued collaboration between scientists, policymakers, and residents is crucial for developing adaptive strategies that protect lives, property, and ecosystems as coastal flood risks increase. According to California's Fourth Climate Change Assessment (Kalansky et al., 2018), adaptive strategies in San Diego must prioritize solutions that address rising sea levels and intensified flooding.

Collecting additional data, such as photographs by lifeguards or city cleanup crews, could improve the precision of these thresholds substantially and better inform local adaptation strategies, including the placement of sandbags and other protective measures. Future research could refine flood impact thresholds and explore the annual and climatic drivers of impactful coastal flooding events. Atmospheric rivers significantly increase the likelihood of photographic evidence of flooding, with nearly four times the odds during an AR event, but the overall correlation between ARs and TWL values is very low. Finally, while ENSO cycles appear to have minimal direct impact on TWL, a more complete dataset could elucidate subtle connections between these climate patterns and coastal flooding.

This study lays a foundation for further investigation into coastal flood risk management. Integrating robust scientific data with community perspectives and expert insights can strengthen evidence-based policies and strategies. Such efforts are essential to safeguarding property, infrastructure, and livelihoods in San Diego County and ensuring a more sustainable, resilient future for coastal communities more generally. Our statistical approach to quantifying flood impact thresholds could, with improved records of impactful coastal flood events, be used to generate action thresholds for decision makers based on modeled and predicted TWL to guide immediate mitigation efforts.

Code and data availability. The datasets supporting the findings of this study are publicly available via Zenodo (DOI: 10.5281/zenodo.18729177). The analysis and figure-generation scripts used in this study are available on Zenodo (DOI: 10.5281/zenodo.18729150).

https://doi.org/10.5194/egusphere-2026-820
Preprint. Discussion started: 6 March 2026

Author Contributions. DMP: Writing (original draft preparation, review and editing), data curation, formal analysis, investigation, methodology, validation, visualization. TWC: Writing (review and editing), conceptualization, data curation, formal analysis, funding acquisition, investigation, methodology, supervision. AC: Writing (original draft), data curation. AG, LE, JF, AG, MM: supervision.

Competing interests. The authors declare no competing interests.

Acknowledgements. The authors would like to recognize funding from the California Nevada Adaptation Program, a NOAA Climate Adaptation Partnership. The authors would like to acknowledge the use of ChatGPT with GPT-4o for editing purposes.

Financial support. This research has been supported by the California Nevada Adaptation Program, a NOAA Climate Adaptation Partnership.

References

Barnard, P. L., Hoover, D., Hubbard, D. M., Snyder, A., Ludka, B. C., Allan, J., Kaminsky, G. M., Ruggiero, P., Gallien, T. W., Gabel, L., McCandless, D., Weiner, H. M., Cohn, N., Anderson, D. L., and Serafin, K. A.: Extreme oceanographic forcing and coastal response due to the 2015–2016 El Niño, *Nature Communications*, 8, 14365, https://doi.org/10.1038/ncomms14365, 2017.

Barnston, A. G., Chelliah, M., and Goldenberg, S. B.: Documentation of a highly ENSO-related SST region in the equatorial Pacific: Research note, Atmosphere-Ocean, 35, 367–383, https://doi.org/10.1080/07055900.1997.9649597, 1997.

Cabrita, P., Montes, J., Duo, E., Brunetta, R., and Ciavola, P.: The role of different total water level definitions in coastal flood modelling on a low-elevation dune system, Journal of Marine Science and Engineering, 12, 1003, https://doi.org/10.3390/jmse12061003, 2024.

California Climate Adaptation Strategy: San Diego Region, State of California: https://climateresilience.ca.gov/regions/san-diego.html, last access: 27 January 2025, n.d.

California King Tides Project: https://www.coastal.ca.gov/kingtides/?os=vbk0&ref=app, last access: 5 March 2026, n.d.

California Sea Level Rise Guidance: 2024 Science and Policy Update, California Sea Level Rise Science Task Force, California Ocean Protection Council, and California Ocean Science Trust, 2024.

CDIP MOP Introduction: https://cdip.ucsd.edu/documents/index/product_docs/mops/mop_intro.html, last access: 17 January 2025, n.d.

Coastal Flooding Viewer-Coastal Processes Group: https://siocpg.ucsd.edu/flood-reporting/coastal-flooding-viewer/, last access: 5 March 2026, 2023.

https://doi.org/10.5194/egusphere-2026-820
Preprint. Discussion started: 6 March 2026

Dettinger, M.: Climate change, atmospheric rivers, and floods in California—A multimodel analysis of storm frequency and magnitude changes, JAWRA Journal of the American Water Resources Association, 47, 514–523, https://doi.org/10.1111/j.1752-1688.2011.00546.x, 2011.

World Meteorological Organization: El Niño / La Niña, https://wmo.int/topics/el-nino-la-nina, last access: 5 March 2026, 2022.

Esri: ArcGIS Pro (Version 3.4.0), Environmental Systems Research Institute, Inc. [software], https://www.esri.com/en-us/arcgis/products/arcgis-pro, 2025.

Fiedler, J. W., Young, A. P., Ludka, B. C., O'Reilly, W. C., Henderson, C., Merrifield, M. A., and Guza, R. T.: Predicting site-specific storm wave run-up, Natural Hazards, 104, 493–517, https://doi.org/10.1007/s11069-020-04178-3, 2020.

Flick, R. E.: A comparison of California tides, storm surges, and mean sea level during the El Niño winters of 1982–83 and 1997–98, Shore & Beach, 66, 7–11, https://escholarship.org/uc/item/6w2284ns, 1998.

Gershunov, A., Shulgina, T., Ralph, F. M., Lavers, D. A., and Rutz, J. J.: Assessing the climate-scale variability of atmospheric rivers affecting western North America, Geophysical Research Letters, 44, 7900–7908, https://doi.org/10.1002/2017GL074175, 2017.

Griggs, G., Cayan, D., Tebaldi, C., Fricker, H. A., Arvai, J., and California Ocean Protection Council Science Advisory Team Working Group: Rising seas in California: an update on sea-level rise science, California Ocean Science Trust, 105–111, https://www.opc.ca.gov/webmaster/ftp/pdf/docs/rising-seas-in-california-an-update-on-sea-level-rise-science.pdf, 2017.

Henny, L. and Kim, K.-M.: The changing nature of atmospheric rivers, Journal of Climate, 38, 1435–1456, https://doi.org/10.1175/JCLI-D-24-0234.1, 2025.

Kalansky, J., Cayan, D., Barba, K., Walsh, L., Brouwer, K., and Boudreu, D.: California's Fourth Climate Change Assessment: San Diego Region Report, CAKE: Climate Adaptation Knowledge Exchange: https://www.cakex.org/documents/california%E2%80%99s-fourth-climate-change-assessment-san-diego-region-report, 2018.

Lindsey, R.: How El Niño and La Niña affect the winter jet stream and U.S. climate, NOAA Climate.gov: http://www.climate.gov/news-features/featured-images/how-el-ni%C3%B1o-and-la-ni%C3%B1a-affect-winter-jet-stream-and-us-climate, last access: 5 March 2026, 2017.

Luna-Niño, R., Gershunov, A., Ralph, F. M., Weyant, A., Guirguis, K., DeFlorio, M. J., Cayan, D. R., and Williams, A. P.: Heresy in ENSO teleconnections: atmospheric rivers as disruptors of canonical seasonal precipitation anomalies in the Southwestern US, Climate Dynamics, 63, 115, https://doi.org/10.1007/s00382-025-07583-1, 2025.

Merrifield, M. A., Johnson, M., Guza, R. T., Fiedler, J. W., Young, A. P., Henderson, C. S., Lange, A. M., O'Reilly, W. C., Ludka, B. C., Okihiro, M., Gallien, T., Pappas, K., Engeman, L., Behrens, J., and Terrill, E.: An early warning system for wave-driven coastal flooding at Imperial Beach, CA, Natural Hazards, 108, 2591–2612, https://doi.org/10.1007/s11069-021-04790-x, 2021.

https://doi.org/10.5194/egusphere-2026-820
Preprint. Discussion started: 6 March 2026

Min, Q., Su, J., Zhang, R., and Rong, X.: What hindered the El Niño pattern in 2014?, *Geophysical Research Letters*, 42, 6762–6770, https://doi.org/10.1002/2015GL064899, 2015.

NOAA California Nevada River Forecast Center (CNRFC): CNRFC storm summaries—late Dec 2022 and Jan 2023, https://www.cnrfc.noaa.gov/storm_summaries/dec2022Jan2023storms.php, last access: 5 March 2026, 2024.

OEHHA: Sea level rise, https://oehha.ca.gov/climate-change/epic-2022/impacts-physical-systems/sea-level-rise, last access: 5 March 2026, 2024.

O'Reilly, W. C., Olfe, C. B., Thomas, J., Seymour, R. J., and Guza, R. T.: The California coastal wave monitoring and prediction system, Coastal Engineering, 116, 118–132, https://doi.org/10.1016/j.coastaleng.2016.06.005, 2016.

Piecuch, C. G., Coats, S., Dangendorf, S., Landerer, F. W., Reager, J. T., Thompson, P. R., and Wahl, T.: High-tide floods and storm surges during atmospheric rivers on the US West Coast, *Geophysical Research Letters*, 49, e2021GL096820, https://doi.org/10.1029/2021GL096820, 2022.

Preston, E.: More powerful storms to hit California, West this weekend, CBS News: https://www.cbsnews.com/news/more-powerful-storms-to-hit-california-west-this-weekend-rain-flooding-damage/, last access: 5 March 2026, 2023.

Quadrado, G. P. and Serafin, K. A.: The timing, magnitude, and relative composition of extreme total water levels vary seasonally along the U.S. Atlantic Coast, Journal of Geophysical Research: Oceans, 129, e2023JC020557, https://doi.org/10.1029/2023JC020557, 2024.

R Core Team: R: A language and environment for statistical computing, R Foundation for Statistical Computing [code], https://www.r-project.org/, 2025.

Ralph, F. M., Neiman, P. J., and Wick, G. A.: Satellite and CALJET aircraft observations of atmospheric rivers over the Eastern North Pacific Ocean during the winter of 1997/98, *Monthly Weather Review*, 132, 1721–1745, https://doi.org/10.1175/1520-0493(2004)132<1721:SACAOO>2.0.CO;2, 2004.

Ralph, F. M., Rutz, J. J., Cordeira, J. M., Dettinger, M., Anderson, M., Reynolds, D., Schick, L. J., and Smallcomb, C.: A scale to characterize the strength and impacts of atmospheric rivers, Bulletin of the American Meteorological Society, 100, 269–289, https://doi.org/10.1175/BAMS-D-18-0023.1, 2019.

Ray, R. D. and Merrifield, M. A.: The semiannual and 4.4-year modulations of extreme high tides, Journal of Geophysical Research: Oceans, 124, 5907–5922, https://doi.org/10.1029/2019JC015061, 2019.

Revell, D., King, P., Giliam, J., Calil, J., Jenkins, S., Helmer, C., Nakagawa, J., Snyder, A., Ellis, J., and Jamieson, M.: A holistic framework for evaluating adaptation approaches to coastal hazards and sea level rise: a case study from Imperial Beach, California, Water, 13, 1324, https://doi.org/10.3390/w13091324, 2021.

Román-Rivera, M. A. and Ellis, J. T.: The king tide conundrum, Journal of Coastal Research, 34, 769–771, 2018.

Serafin, K. A., Ruggiero, P., and Stockdon, H. F.: The relative contribution of waves, tides, and nontidal residuals to extreme total water levels on U.S. West Coast sandy beaches, *Geophysical Research Letters*, 44, 1839–1847, https://doi.org/10.1002/2016GL071020, 2017.

https://doi.org/10.5194/egusphere-2026-820
Preprint. Discussion started: 6 March 2026

Shields, C. A., Li, H., Castruccio, F. S., Fu, D., Nardi, K., Liu, X., and Zarzycki, C.: Response of the upper ocean to northeast Pacific atmospheric rivers under climate change, Communications Earth & Environment, 5, 603, https://doi.org/10.1038/s43247-024-01774-0, 2024.

SIO Coastal Processes Group: January 6, 2023 coastal flooding event recap, ArcGIS StoryMaps: https://storymaps.arcgis.com/stories/e0b3d1724b474b05bf3f932fda7d334d, last access: 5 March 2026, 2023.

Station Home Page—NOAA Tides & Currents: https://tidesandcurrents.noaa.gov/stationhome.html?id=9410230, last access: 5 March 2026, n.d.

Stockdon, H. F., Holman, R. A., Howd, P. A., and Sallenger, A. H.: Empirical parameterization of setup, swash, and runup, Coastal Engineering, 53, 573–588, https://doi.org/10.1016/j.coastaleng.2005.12.005, 2006.

Sweet, W., Dusek, G., Obeysekera, J. T. B., and Marra, J. J.: Patterns and projections of high tide flooding along the U.S. coastline using a common impact threshold, NOAA Technical Report NOS CO-OPS 086, NOAA, Silver Spring, MD, 2018.

Thompson, P. R., Widlansky, M. J., Hamlington, B. D., Merrifield, M. A., Marra, J. J., Mitchum, G. T., and Sweet, W.: Rapid increases and extreme months in projections of United States high-tide flooding, Nature Climate Change, 11, 584–590, https://doi.org/10.1038/s41558-021-01077-8, 2021.

Tseng, K.-C. and Johnson, N.: When rivers reach the sky, NOAA Climate.gov: http://www.climate.gov/news-features/blogs/enso/when-rivers-reach-sky, last access: 5 March 2026, 2022.

Wing, O. E. J., Lehman, W., Bates, P. D., Sampson, C. C., Quinn, N., Smith, A. M., Neal, J. C., Porter, J. R., and Kousky, C.: Inequitable patterns of US flood risk in the Anthropocene, Nature Climate Change, 12, 156–162, https://doi.org/10.1038/s41558-021-01265-6, 2022.

Xia, R.: California against the sea: visions for our changing coastline, Heyday, 2023.

Younger, S.: NASA-led study pinpoints areas sinking, rising along California coast, NASA Jet Propulsion Laboratory, https://www.jpl.nasa.gov/news/nasa-led-study-pinpoints-areas-sinking-rising-along-california-coast/, last access: 5 March 2026, 2025.

Zhu, Y. and Newell, R. E.: A proposed algorithm for moisture fluxes from atmospheric rivers, Monthly Weather Review, 126, 725–735, https://doi.org/10.1175/1520-0493(1998)126<0725:APAFMF>2.0.CO;2, 1998.